17B.7

A NUMERICAL AND ANALYTICAL STUDY OF INTERMITTENCY IN THE STABLE BOUNDARY LAYER

Wiet de Ronde, Harm J. J. Jonker*
Multi-Scale Physics, Delft University of Technology, The Netherlands
Bas van de Wiel, Arnold Moene
Meteorology and Air Quality Section, Wageningen University, The Netherlands

Abstract

This paper studies the phenomenon of intermittency in the stable boundary layer with particular emphasis on the energetic coupling between land and atmosphere. The stable boundary layer is modelled with two different minimalistic models, a one-dimensional (height-dependent) model and a bulk model. Turbulence is parameterized using a Richardson number dependent eddy viscosity. The most important ingredient of both models is the treatment of the lower boundary: it is based on a simplified energy balance of a vegetation layer and includes besides radiative cooling an energetic coupling with both the atmosphere and the deep soil. The resulting temperature boundary condition is time-dependent and interacts with the atmospheric dynamics.

For a large range of parameters both models display unsteady behaviour where the state of the atmosphere changes between turbulent and laminar (collapsed turbulence). But sustained unsteady behaviour appears only possible when the coupling between vegetation and atmosphere is sufficiently strong. Both models show qualitative comparable behaviour. This provides a strong indication that the surface-atmosphere interaction could play an important role in the occurrence of intermittency in the stable boundary layer.

1. INTRODUCTION

In the diurnal cycle the atmospheric boundary layer undergoes a transition from an unstable daytime boundary layer to a stable nighttime boundary layer. Two types of stable boundary layer are defined (Mahrt, 1999)

- the Weakly Stable Boundary Layer
- the Very Stable Boundary Layer

In the weakly continuous boundary layer turbulence intensity is continuously present and the boundary layer can be described by local similarity scaling (Nieuwstadt, 1984). The very stable boundary layer occurs on clear nights with weak winds, where due to long-wave radiation the surface cools strongly. Due to the resulting strong stratification, turbulent intensity is very low or completely absent. In field experiments often an intermittent form of turbulence is observed with a marked temporal change in turbulence intensity. This intermittency is of a global form, in a sense that the turbulence intensity on all length scales is either present or (completely) suppressed (Howell and Sun, 1999; Doran, 2004; Salmond, 2005; van de Wiel et al., 2003). The mechanism(s) that drive this form of intermittent turbulence are currently not fully understood. Suggested mechanisms that drive intermittent behaviour are density currents, solitons (Sun et al., 2004), gravity waves (Einaudi and Finnigan, 1993), a non-stationair mean flow (Cullen et al., 2007) or surface heterogeneity (Nakamura and Mahrt, 2005). These proposed mechanisms can be qualified as having a non-local (external) origin. Other suggestions include low level jets (Smedman, 1988) and Ekman layer instabilities (Barnard, 2000). These suggestions are based on the influence of the Coriolis force to create instabilities in the flow. However, one could argue that the characteristic time scale of the Coriolis force is longer than the characteristic time scale of intermittent events (ReVelle, 1993).

For this reason it is interesting to focus on local (internal) mechanisms that drive intermittency. A simple local model was first proposed by Businger (1973). The stratification in the boundary layer due to the cooling suppresses turbulence resulting in a laminar flow. Because turbulent friction is absent, this flow accelerates, which ultimately leads to the re-occurence of turbulence due to the increased shear stresses. Turbulent mixing then reduces the shear stresses while the stratification due to ongoing cooling drives the flow back into a laminar state. This cycle can continue during the night. Blackader (1979) suggested that the dynamics due to land surface - atmosphere interaction could lead to intermittent events using a simple 1-dimensional model. Comparable results were obtained by ReVelle (1993) and van de Wiel et al. (2002b) for respectively a 1D model and a bulk model. It is important that the land-atmosphere interaction is dynamic. A fixed surface temperature, or a fixed surface flux $(\overline{w'T'})$ is unlikely to be sufficient for intermittency to occur, since the system will favor either the turbulent or laminar state without switching. A land-atmosphere interaction scheme therefore should incorporate physically realistic cooling and heating terms. As argued by van de Wiel et al. (2002b) even simple models of the land-atmosphere interaction should be based on the energy balance of the surface, taking into account cooling by radiation, the heat flux to/from the deeper soil layers, and an energetic coupling with atmosphere.

In this paper we pursue these ideas in modelling the stable boundary layer. We study a one-dimensional

* *Corresponding author address:* Harm Jonker, Dept. of Multi-Scale Physics, Delft University of Technology, Delft, The Netherlands (h.j.j.jonker@tudelft.nl - www.msp.tudelft.nl)

model in which the turbulence transport terms are modeled by an eddy-diffusivity closure. To get a better qualitative understanding of the cause of intermittency, we simplify the model further to a bulk model. We show that within both frameworks the interactive coupling between land and atmosphere is a crucial ingredient for intermittent behaviour to occur.

2. GOVERNING EQUATIONS

Using a pressure gradient as driving force, and neglecting molecular transport and the Coriolis force, one finds the following governing equations for the ensemble mean horizontal velocity $U(z,t)$ and temperature $T(z,t)$ (e.g. (Nieuwstadt, 2005))

$$\frac{\partial U}{\partial t} = -\frac{1}{\rho}\frac{dP}{dx} - \frac{\partial}{\partial z}\left(\overline{u'w'}\right) \tag{1a}$$

$$\frac{\partial T}{\partial t} = -\frac{\partial}{\partial z}\left(\overline{w'T'}\right) \tag{1b}$$

where $\overline{u'w'}$ and $\overline{w'T'}$ are the turbulent transport terms. To close the set of equations we use the Richardson number closure commonly applied in stable boundary layers

$$\overline{u'w'} = -K_M\frac{\partial U}{\partial z} \tag{2}$$

$$\overline{w'T'} = -K_H\frac{\partial T}{\partial z} \tag{3}$$

where the eddy-viscosity/diffusivity is given by

$$K_M = K_H = (\kappa z)^2 f(Ri)\left|\frac{\partial U}{\partial z}\right| \tag{4}$$

with $\kappa = 0.4$ the Von Karman constant and $f(Ri)$ given by

$$f(Ri) = \begin{cases} \left(1-\frac{Ri}{Ri_c}\right)^2, & \text{for } 0 \le Ri \le Ri_c \\ 0, & \text{otherwise.} \end{cases} \tag{5}$$

Here Ri is the gradient Richardson number, defined as

$$Ri = \frac{g}{T_0}\frac{\frac{\partial T}{\partial z}}{\left(\frac{\partial U}{\partial z}\right)^2} \tag{6}$$

where $g\ \left[m\,s^{-2}\right]$ is the gravitational acceleration and $T_0 = 300K$ is a reference temperature. Ri_c is the critical Richardson number. As a consequence of (5), for $Ri(z) > Ri_c$ stratification suppresses turbulence completely. In contrast, turbulent eddies are always (locally) present at height z when $Ri(z) < Ri_c$. The value of Ri_c is experimentally observed to be $Ri_c = \frac{1}{5.2}$ (Webb, 1970), but for simplicity we take $Ri_c = \frac{1}{5}$. For $Ri_c = \alpha^{-1}$ the closure (4) is consistent (e.g. van de Wiel et al. (2002b, 2008)) with the surface layer similarity functions for the stable boundary layer, which are given by the loglinear flux-profile relation

$$\frac{\kappa z}{u_*}\frac{\partial U}{\partial z} = \phi\left(\frac{z}{L}\right) = 1 + \alpha\frac{z}{L} \tag{7}$$

where L is the Obukhov length scale, defined as

$$L = \frac{u_*^3}{\kappa\frac{g}{T_0}\left[u_*T_*\right]} \tag{8}$$

with u_* is the surface friction velocity and $[u_*T_*] = \overline{w'T'}(z=0)$ the surface heat flux.

2.1 *Boundary conditions*

At the top of our domain we use for the velocity a free-slip condition for U and a constant temperature T_{top} which we can set to zero without loss of generality. At the surface we follow a land-atmosphere interaction approach, following Blackader (1957); ReVelle (1993); van de Wiel et al. (2002b) which is based on the energy balance of a vegetation layer. It includes radiative cooling, a heat-flux to/from the deep soil, and a heat-flux coupling with atmosphere. The resulting equation is

$$\frac{\partial T_{\text{veg}}}{\partial t} = -\frac{T_{\text{veg}}-\tilde{T}_g}{\tau} - \frac{Q}{\rho_v c_{pv}\delta} + \frac{\beta}{\delta}\left(K_H\frac{\partial T}{\partial z}\right)_{z=0} \tag{9}$$

where $\tilde{T}_g\ [K]$ is the temperature of the deep ground , $\tau\ [s]$ is a timescale for heat transport between the vegetation layer and the deep ground and $\beta\ [-]$ is the ratio of the heat capacities of air and the vegetation layer, $\delta\ [m]$ the height of the vegetation layer, and Q the radiative cooling $\left[W/m^2\right]$. One may note that the radiative cooling term can be mathematically absorbed in the ground temperature by defining $T_g = \tilde{T}_g - \tau Q/\rho_v c_{pv}$, which reduces the number of parameters. This equation then consists of two terms, a vegetation 'heating' term $\left(\beta\delta^{-1}\left[K_H\partial T/\partial z\right]_{z=0}\right)$, which is dependent on the state (turbulent or laminar) of the atmosphere through K_H, and a 'cooling' term $\left(-\tau^{-1}\left[T_{\text{veg}}-T_g\right]\right)$, which drives T_{veg} towards T_g. We now take $T(0) = T_{\text{veg}}(t)$, resulting in a time-dependent surface boundary condition. The total set of equations

$$\frac{\partial U}{\partial t} = -\frac{1}{\rho}\frac{\partial P}{\partial x} + \frac{\partial}{\partial z}\left[K_M\frac{\partial U}{\partial z}\right] \tag{10}$$

$$\frac{\partial T}{\partial t} = \frac{\partial}{\partial z}\left[K_H\frac{\partial T}{\partial z}\right] \tag{11}$$

$$\frac{\partial T_{\text{veg}}}{\partial t} = -\frac{T_{\text{veg}}-T_g}{\tau} + \gamma\,K_H\frac{\partial T}{\partial z}\bigg|_{z=0} \tag{12}$$

with K_H and K_M from (4) and $\gamma = \beta/\delta$. In section 4 we study the time dependent behaviour of this system in greater detail. As we will see there, the behaviour of this relatively simple model is already very complex, which hampers a good understanding of the phenomena. For this reason we derive in the next section an even simpler model which shows conceptually what is going on.

3. INTERMITTENCY IN THE BULK MODEL

In the bulk model the governing partial differential equations (10-11) are integrated over the domain height resulting in a set of ordinary differential equations for the

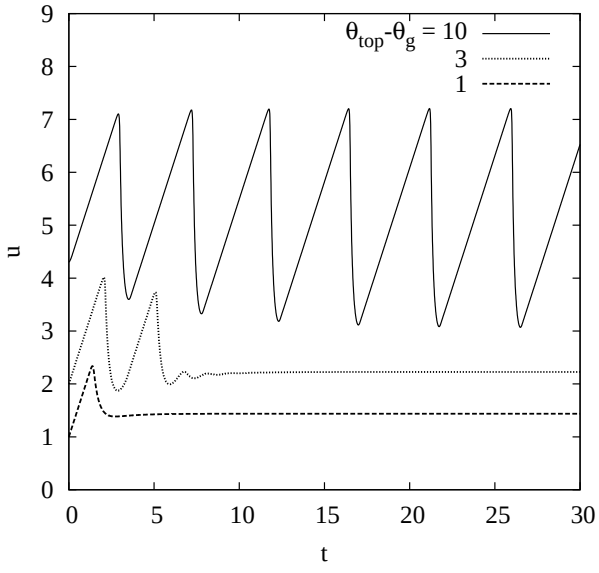

(a)

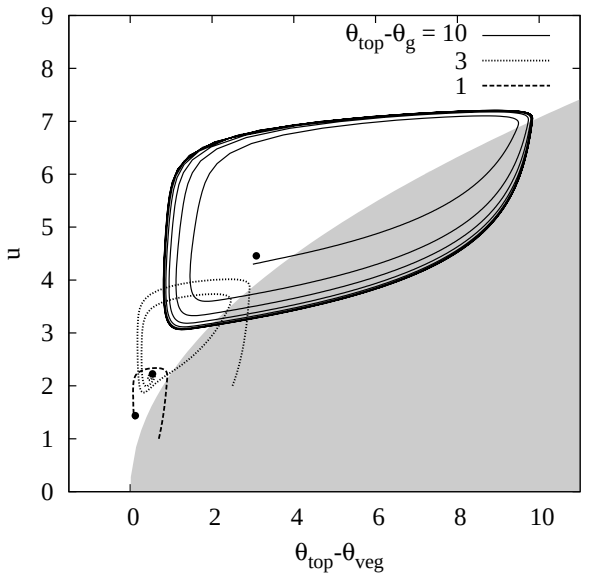

(b)

Figure 1: a) Time-series of u in the bulk-model for different values of the temperature difference $\theta_{\rm top} - \theta_{\rm g}$. The parameters $\alpha = 10$ and $\tau = 1$ are fixed. b) Corresponding trajectories in phase-space $u(t)$ vs $\theta_{\rm top} - \theta_{\rm veg}(t)$. The shaded area represents the region where $Ri > Ri_c$. Dots indicate the fixed-point associated with the value of the temperature difference $\theta_{\rm top} - \theta_{\rm g}$ as given by (19-21).

domain-averaged values of velocity $\langle U \rangle$, and temperature $\langle T \rangle$, in combination with the equation for the vegetation temperature $T_{\rm veg}$. We discretize the system such that K_M, K_H are located at $z = H/2$, together with $\langle U \rangle$, and $\langle T \rangle$. With regard to the boundaries, we use a free-slip top-boundary condition and a no-slip bottom boundary condition, while for the temperature we have a fixed top temperature T_{top} and the *interactive* bottom temperature $T_{\rm veg}\,(t)$. The relevant gradients can then be approximated by $\frac{\partial U}{\partial z}\big|_{z=0} = \frac{\langle U \rangle}{H/2}$, $\frac{\partial T}{\partial z}\big|_{z=0} = \frac{\langle T \rangle - T_{\rm veg}}{H/2}$, $\frac{\partial T}{\partial z}\big|_{z=H} = \frac{T_{top} - \langle T \rangle}{H/2}$, which yields

$$\frac{d\langle U \rangle}{dt} = -\frac{1}{\rho}\frac{\partial P}{\partial x} - \frac{2K_M}{H^2}\langle U \rangle \quad (13)$$

$$\frac{d\langle T \rangle}{dt} = \frac{2K_H}{H^2}\left[T_{top} - 2\langle T \rangle - T_{\rm veg}\right] \quad (14)$$

$$\frac{dT_{\rm veg}}{dt} = -\frac{T_{\rm veg} - T_g}{\tau} + \frac{2\gamma K_H}{H}(\langle T \rangle - T_{\rm veg}) \quad (15)$$

The eddy diffusivities are again closed by equation (4), with $z = H/2$. With the adopted discretization the Richardson number (6) becomes $Ri = gH(T_{top} - T_{\rm veg})/(4T_0\langle U \rangle^2)$. The equations can be simplified further by scaling the variables; if we take $\mathcal{U} = \kappa^{-1}\sqrt{-\frac{1}{\rho}\frac{\partial P}{\partial x}H}$ the velocity-scale, $H/(\kappa^2\mathcal{U})$ the time-scale, and $\mathcal{T} = 4T_0\mathcal{U}^2/gH$ the temperature-scale, we derive for the system in dimensionless form

$$\frac{du}{dt} = 1 - u^2 f(Ri) \quad (16)$$

$$\frac{d\theta}{dt} = (\theta_{\rm top} - 2\theta + \theta_{\rm veg})\, u f(Ri) \quad (17)$$

$$\frac{d\theta_{\rm veg}}{dt} = -\frac{\theta_{\rm veg} - \theta_{\rm g}}{\tau} + 2\alpha(\theta - \theta_{\rm veg})\, u f(Ri) \quad (18)$$

where $f\,(Ri)$ is described by equation (5) with $Ri = (\theta_{\rm top} - \theta_{\rm veg})/u^2$. As such the model is even more rudimentary than the bulk-model derived by van de Wiel et al. (2002b). The justification for this is that the present approach focusses entirely on the role of the vegetation-atmosphere interaction and much less on describing the energetics of the vegetation layer very accurately. The dimensionless parameter $\alpha = H\gamma/2$ thus plays a key role in this model since it represents the interaction between atmosphere and vegetation. For $\alpha = 0$ the vegetation temperature does not depend on the atmospheric temperature. Note that τ is now dimensionless as well. Treating $Ri_c = 0.2$ as a given fixed value, the system essentially has three independent dimensionless parameters α, τ, and $\theta_{\rm top} - \theta_{\rm g}$ which is the temperature difference over the entire domain. Without loss of generality one could set $\theta_{\rm top} = 0$ because all temperatures can be shifted by a constant value without changing the system, but for clarity we prefer the notation $\theta_{\rm top} - \theta_{\rm g}$ over $-\theta_{\rm g}$. Analysis of the three-dimensional system (16-18) reveals that there is a only one possible stationary state, which

depends on the three parameters as

$$\hat{u} = \frac{1-\alpha\tau}{2} + \sqrt{\left(\frac{1+\alpha\tau}{2}\right)^2 + \frac{\theta_{\rm top}-\theta_{\rm g}}{Ri_c}} \quad (19)$$

$$\hat{\theta} = \frac{\theta_{\rm top}+\hat{\theta}_{\rm veg}}{2} \quad (20)$$

$$\hat{\theta}_{\rm veg} = \theta_{\rm top} - (\theta_{\rm top}-\theta_{\rm g})\frac{\hat{u}}{\hat{u}+\alpha\tau} \quad (21)$$

In the neutral situation $\theta_{\rm g} = \theta_{\rm top}$, the stationary state is $\hat{u} = 1$, and $\hat{\theta} = \hat{\theta}_{\rm veg} = \theta_{\rm top}$, regardless of the values of α and τ. However, when there is a temperature difference $\theta_{\rm top} - \theta_{\rm g} > 0$, the equilibrium velocity will increase, i.e. $\hat{u} > 1$, owing to the less efficient turbulent mixing of momentum in the stably stratified situation (lower K_M). One may further note that in this situation the equilibrium state does depend on two parameters rather than three, i.e. the temperature difference $\theta_{\rm top} - \theta_{\rm g}$ and the product $\alpha\tau$. This means that for the stationary state there is a trade-off between the land-atmosphere coupling α and the soil response time τ.

Note that the stationary states (19-21) do not comprise the decoupled state where $Ri > Ri_c$ and $K_M = 0$. The inadmissibility of this solution as a stationary state is a direct consequence of our choice to force the system by a constant pressure gradient: when $Ri > Ri_c$, $f(Ri) = 0$ by which equation (16) becomes $du/dt = 1$; this implies that $u(t)$ will grow linearly until $Ri = (\theta_{\rm top} - \theta_{\rm veg})/u^2$ drops below the critical value Ri_c. This is inevitable because $\theta_{\rm veg}$ is bounded – it cannot become smaller than $\theta_{\rm g}$ –, whereas u will grow unbounded when $Ri > Ri_c$. In line with this argument, one may verify that the *stationary state* Richardson-number $\hat{Ri} = (\theta_{\rm top} - \hat{\theta}_{\rm veg})/\hat{u}^2$ is always below Ri_c.

It is however important to realize that the fixed-point (19-21) might not be stable at all. Since under the dynamics of (16-18) none of the variables u, θ, $\theta_{\rm veg}$ can escape to $\pm\infty$, instability of the (only) fixed-point solution must entail non-trivial behaviour such as chaos or limit-cycles. In Fig. 1 we show the timeseries for three values of the global temperature difference $\theta_{\rm top} - \theta_{\rm g} = 1, 3$ and 10, while $\alpha = 10$ and $\tau = 1$ are fixed. For a small temperature difference the solutions rapidly converge to the fixed-point solution. For moderate temperature differences $\theta_{\rm top} - \theta_{\rm g}$ the variables reach the equilibrium value in an oscillatory fashion. For a relatively large temperature difference $\theta_{\rm top} - \theta_{\rm g}$ the fixed-point is no longer stable; it spirals away from it and settles into a limit cycle. The phasespace trajectories in Fig. 1b show that one branch of the cycle is always in the turbulent state and the other in the decoupled state (indicated by the gray zone which represents $Ri > Ri_c$).

In order to get more insight in the stability of the fixed-point and in the transition from stationary to unsteady behaviour, we study the eigenvalues of Jacobian matrix evaluated at the fixed-point $(\hat{u}, \hat{\theta}, \hat{\theta}_{\rm veg})$ which after some

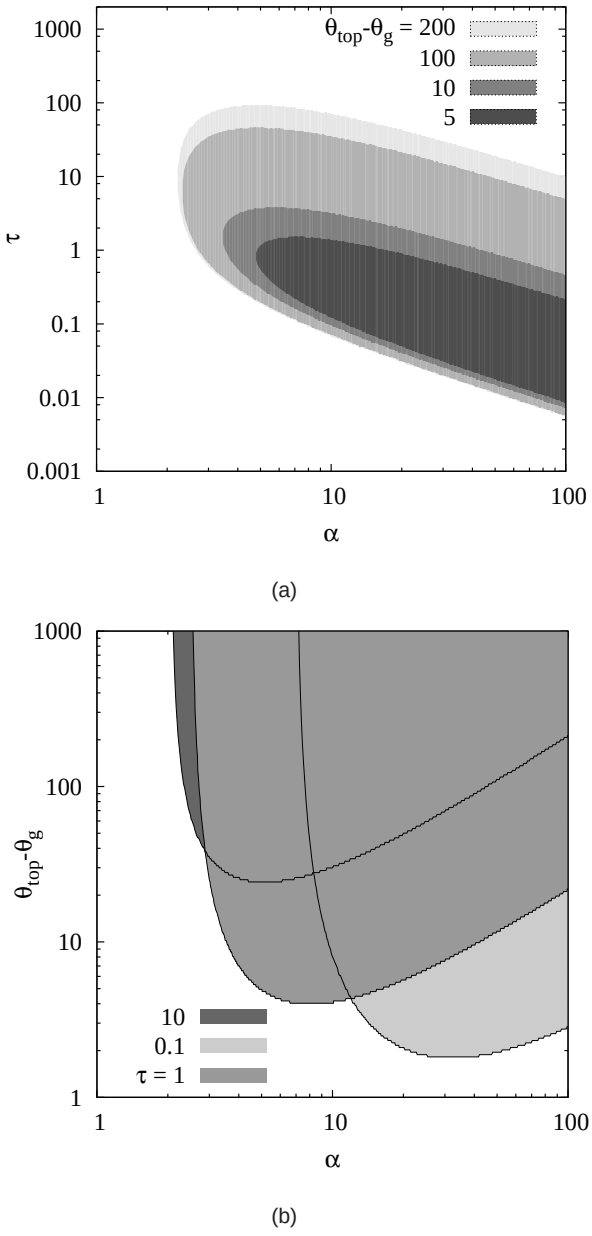

Figure 2: Regime-plots indicating the stability of the fixed-point solutions (19-21). Shaded regions represents the parameter regime where one of the eigenvalues of the Jacobian (22) has a positive real part. At the perimeter of the regions the system undergoes a Hopf-bifurcation; inside the regions the system is has a periodic solution (limit-cycle).

manipulation reads

$$J = \begin{pmatrix} -\frac{2}{\hat{u}} - \frac{4\hat{R}i}{Ri_c} & 0 & -\frac{2}{\hat{u}Ri_c} \\ 0 & -\frac{2}{\hat{u}} & \frac{1}{\hat{u}} \\ \alpha\hat{R}i + \frac{4\alpha\hat{R}i^2\hat{u}}{Ri_c} & \frac{2\alpha}{\hat{u}} & -\frac{1}{\tau} - \frac{2\alpha}{\hat{u}} + \frac{2\alpha\hat{R}i}{Ri_c} \end{pmatrix} \tag{22}$$

For a large range of parameter values we have calculated the eigenvalues of J and located the parameter regime where at least one of the eigenvalues has a positive real value, which indicates that the fixed-point is linearly unstable. The results have been plotted in Fig.2, where a shaded region indicates instability of the fixed-point. Since as mentioned the system cannot escape to infinity and since no chaotic solutions were observed, a shaded region indicates that the system has a periodic solution. At the region-perimeter the system undergoes a Hopf-bifurcation, since there the real part of the (complex) eigenvalues changes sign.

The other relevant point to notice in Fig.2 is that unsteady solutions cannot exist when the coupling parameter α is below a critical value. Indeed, for α smaller than roughly 2, no combinations of τ and $\theta_{\mathrm{top}} - \theta_{\mathrm{g}}$ can be found such that the fixed point is unstable. This clearly shows that, within the adopted framework, a non-vanishing land-atmosphere interaction is a necessary condition for intermittency to happen.

4. INTERMITTENCY IN THE ONE-DIMENSIONAL MODEL

In the 1-dimensional model, described by equations 10-12, we implement a $z0$-concept to model the influence of the rough surface on the flow. The actual boundary is at $z = (h)$, with $h/H = 0.02$. Integrating the log-linear flux-gradient relations from 0 to h one obtains at $z = h$

$$u_* = \kappa U(h) \left(\ln\left(\frac{h}{z_0}\right) + \frac{h - z_0}{Ri_c L} \right)^{-1} \tag{23a}$$

$$T_* = \kappa \triangle T(h) \left(\ln\left(\frac{h}{z_0}\right) + \frac{h - z_0}{Ri_c L} \right)^{-1} \tag{23b}$$

where u_*^2 is the momentum flux and $u_* T_*$ is the heat flux at $z = z_0$. Using the definition of the height z_0, we have $U(z_0) = 0$ and $\triangle T(h) = T(h) - T(z_0)$. We obtain the value for $T(z_0)$ from the vegetation layer model (9), i.e. $T(z_0) = T_{\mathrm{veg}}(t)$. Using (23) and (8) we note the positive feedback between the Obukhov length L $\left(L = u_*^3 \left[\kappa g (u_* T_*)/T_0\right]^{-1}\right)$ and u_*, in the sense that an increase in u_* leads to an increase in L which leads to an increase in u_*. In contrast, a negative feedback exists between $U(h)$ and u_*.

We numerically solve the 1D-model using a staggered grid with 400 cells, where we define U and T on cell centers and fluxes (e.g. $-K_M \partial U/\partial z$) on cell boundaries. At the top we take a free-slip condition for velocity and a fixed temperature condition (T_{top}) for T, which we set to zero without loss of generality. In the simulations we simulate a night of 8 hours, from sunset to sunrise. The initial state of the model is a neutral log-profile for $U(z)$, $K(z) = (\kappa z)^2 |\partial U/\partial z|$, and $T_{\mathrm{veg}} = T(z) = 0$. The time-integration scheme is direct Euler-forward with a fixed timestep $\triangle t = 5 \times 10^{-4}\, s$.

The scaling variables employed in the bulk model are not suitable in the 1D-model because the height of the domain (H) is not the boundary layer height and therefore not a characteristic length scale. We therefore show the results in dimensional notation. Another important issue that should be addressed is the absence of any mixing when $Ri(z) \geq Ri_c$. This has two important consequences. First, a sharp bend exists in the profiles at the transition from $Ri < Ri_c \rightarrow Ri > Ri_c$. Second, the information in the turbulent regions (close to the surface) where $Ri(z) < Ri_c$ is not transported over this Ri-transition. In this region $(Ri(z) > Ri_c)$ initial gradients are directly removed by turbulent mixing and a laminar flow develops, undisturbed by unsteady behaviour near the surface. A consequence of this is a slight grid dependency during unsteady behaviour. In simulations without unsteady behaviour no grid dependency is observed. Because the only influence of an increase in grid cells is a slight temporal shift in the unsteady dynamics, it is reasonable to assume that the main characteristics of the unsteady behaviour do not depend on the employed resolution.

In the simulations we observe three different types of nights. The first type, the radiative night, is characterized by strong stratification, leading to a negligible heat flux from the atmosphere to the vegeation by which $T_{\mathrm{veg}} \rightarrow T_g$. The second type, a turbulent night, has a large atmospheric heat flux such that $T_{\mathrm{veg}} \approx 0$. Finally, nights exist, where these two states are interchanged, the intermittent nights. These three types of nights are also observed in field measurements (e.g. van de Wiel et al. (2002a, 2003)). These three types of nights can be explained by noting the dynamical behaviour of T_{veg} (equation 12). For strong cooling, $f(Ri) = 0$ and the heating term is negligible compared to the cooling term. For a strong turbulent night, $f(Ri) > 0$ and either τ is large or $T_{top} - T_g$ is small, leading to an atmospheric heat flux to the vegetation capable of balancing the cooling term. However, in between these two states the relative influence of both terms is important. The characteristic response time τ of the vegetation to the deep soil temperature (in which we absorbed the radiative term) and γ the coupling coefficient of the atmospheric flux with the vegetation , dominate the process. For very large τ the response is slow for changes in the state of the atmosphere and longer timescales for unsteady behaviour are expected. In figure 3 we show these different types of nights, for varying values of γ and τ.

Since in this study we are particularly interested in the dynamical interaction of the vegetation layer and the state of the atmosphere, we focus on the intermittent behaviour where the laminar and turbulent state are interchanged. In figures 4 and 5 we show the time series of T_{veg} and the ground-flux $\left(-\tau^{-1}(T_{\mathrm{veg}} - T_g)\right)$ and atmospheric flux $(\gamma u_* T_*)$. The intermittent behaviour is aperi-

odic, both in amplitude and period, and tends to decay on large time-scales. These trends are observed in most of our simulations.

Direct after sunset, due to the 'cooling' term, T_{veg} exponentially approximates T_g. The system moves into a stratified regime $(L \to 0)$ and the surface fluxes $\left(u_* T_* \text{ and } u_*^2\right)$ vanish. The system is uncoupled, in the sense that the heat- and momentum-transfer between vegetation and atmosphere is negligible. Due to the suppression of surface friction the atmospheric flow accelerates, where the relative velocity increase is larger near the surface. At a critical point the further increase of $U(h)$ initiates the very rapid positive feed-back loop between L and u_* and a large turbulence burst occurs.

Indeed we can rewrite equations 23 and use that $u_*/T_* = \triangle U/\triangle T = U(h)/(T(h) - T_{\mathrm{veg}})$ to derive after some rearrangement

$$u_*^2 = \left[\ln\left(\frac{h}{z_0}\right)\right]^{-2} (\kappa \triangle z)^2 \left(\frac{\triangle U}{\triangle z}\right)^2 \left(1 - \frac{Ri_{\triangle}}{Ri_c}\right)^2 \quad (24)$$

where $\triangle z = h - z_0$ and

$$Ri_{\triangle} = \frac{g}{T_0} \frac{\frac{\triangle T}{\triangle z}}{\left(\frac{\triangle U}{\triangle z}\right)^2} \quad (25)$$

and the critical point can be identified with the point when $Ri_{\triangle} < Ri_c$. The soil flux, governed by τ, always lags the atmospheric flux. An increase in the total heat flux is the result.

During the turbulence burst the system re-couples. The direct consequences of this coupling are the increase of both the surface heat flux and the surface friction velocity. The increase of the surface heat flux $(u_* T_*)$ has a positive effect on T_{veg} and a negative effect on $T(h)$. On a somewhat longer timescale, the turbulent eddies enhance the mixing in the atmosphere, leading to an entrainment flux of warm air from higher regions (figures 6 and 7). This entrainment causes the rise in temperature during the turbulence burst. The height averaged temperature of the system decreases with every cycle.

The surface friction velocity is negatively coupled to $\triangle U$ since the turbulence causes additional friction. Hence $\triangle U$ decreases, $Ri_{\triangle} > Ri_c$, and the turbulence collapses. We return to the decoupled situation where the cooling is dominated by T_g and T_{veg} decreases. We can now summarize the influence of a single turbulence burst on our dynamical system. First, the mixing of air in the atmosphere leads to entrainment of warmer air down. As a result the height of the laminarized layer grows in time (see figures 8 and 9). Because the laminarized region is larger after every single burst, the duration of a burst is longer in subsequent bursts. The turbulence grows from the surface towards the inversion and the total time of this process is height dependent. Second, the heat flux from the atmosphere to the vegetation layer leads to a gradual decrease of the atmospheric temperature, $(T(z))$. The temperature difference $(\triangle T)$ becomes smaller with every single burst. The stratification strength decreases and turbulence persists longer, eventually leading to a continuously weakly turbulent state.

In figure 10 we show a plot comparable to figure 2a. The shaded regions are the ranges where intermittent behaviour is observed. The qualitative similarity is striking. First, the general shape of the regions is similar. Second we observe for the coupling parameter γ a critical minimum value below which there is no unsteady behaviour. In a quantitative sense the results are of course not directly comparable: In contrast to the bulk model we do calculate the stability of solutions analytically. Rather, in the 1D model we define a maximum integration time (8 hours) and unsteady behaviour with a transient period longer than this time is not represented in the graph (e.g. in the bottom left figure of figure 3 one could argue that the integration time is too short). Second, in the 1D model the depth of the stable boundary layer increases. This complicates the direct comparison of the ranges for τ and γ between the 1D model and the bulk model.

The parameter τ is a measure for the response time of vegetation to the deep ground temperature. A very large value of τ corresponds to a low thermal diffusivity of the ground. For grasslands $\tau \approx \mathcal{O}\left(10^2\right) \sim \mathcal{O}\left(10^3\right)$, which would be comparable to our results. γ is the energetic coupling coefficient between vegetation and atmosphere. It depends on the ratios of the volumetric heat capacities (β), divided by the height of the vegetation layer δ. The height of vegetation layer we assume $\mathcal{O}\left(10^{-2}\right)$ and for air the volumetric heat capacity is $(\rho c_p)_a = \mathcal{O}\left(10^3\right)$ we have $(\rho c_p)_v = \mathcal{O}\left(10^4\right)$ for $\beta = \mathcal{O}(10)$. Finally, T_g was defined as the mathematical contraction between the deep ground temperature and constant net radiative forcing.

$$T_g = \tilde{T}_g - \frac{Q\tau}{(\rho c_p)_v \delta} \quad (26)$$

where $\tilde{T}_g$ is the real ground temperature and Q is the long-wave radiation. If we take $\tilde{T}_g = 0$ we have

$$Q = \frac{(\rho c_p)_v \delta T_g}{\tau} = \frac{\mathcal{O}\left(10^{-2}\right)\mathcal{O}\left(10^4\right)\mathcal{O}(10)}{\mathcal{O}\left(10^2\right)} = \mathcal{O}(10) \quad (27)$$

which, given the above rough estimates, is not unrealistically far from measured radiation values $\left(Q \approx 60 \sim 100\, W/m^2\right)$.

5. CONCLUSIONS AND DISCUSSION

Using two minimalistic approaches, a bulk model and a 1D model, the stable boundary layer is modelled. Both models show unsteady behaviour for a wide range of parameters. Furthermore, the types of behaviour observed in this conceptual study (turbulent, radiative and intermittent) are comparable to observations in field experiments. Within the adopted framework, the role of the land-atmosphere coupling turned out be crucial.

Both models are obviously rather crude. They are based on a rigid turbulence parameterization (equation 5, where the presence of turbulence is a prescribed function

of Ri. In addition, the precise details of the heat transfer between the vegetation layer and both atmosphere and soil have been only conceptually accounted for. Also the absence of Coriolis force in our model is unrealistic. On the other hand, the results show that the Coriolis force is not a prerequisite for intermittency; also the land-atmosphere interaction could be responsible. We stress that the mechanism studied in this paper does not rule out any other mechanism for intermittency.

ACKNOWLEDGMENTS

This work was sponsored by the Stichting Nationale Computerfaciliteiten (National Computing Facilities Foundation, NCF), with financial support from the Nederlandse Organisatie voor Wetenschappelijk Onderzoek (Netherlands Organization for Scientific Research, NWO).

References

Barnard, J., 2000: Intermittent turbulence in the very stable ekman layer. Ph.D. thesis, University of Washington.

Blackader, A., 1957: Boundary-layer wind maxima and their significance for the growth of nocturnal inversions. *Bulletin of the American Meteorological Society*.

Blackader, A., 1979: High resolution models of the planetary boundary layer. *Advances in Environmental Science and Engineering*, 50–85.

Businger, J., 1973: Turbulent transfer in the atmospheric surface layer. *American Meteorological Society*, workshop of Micrometeorology.

Cullen, N., K. Steffen, and P. Blanken, 2007: Nonstationarity of turbulent heat fluxes at summit, greenland. *Boundary-Layer Meteorology*, **122**, 439–455.

Doran, J., 2004: Characteristics of intermittent turbulent temperatrue fluxes in stable conditions. *Boundary-Layer Meteorology*, **112**, 241–255.

Einaudi, F. and J. Finnigan, 1993: Wave-turbulence dynamics in the stably stratified boundary layer. *Journal of the Atmospheric Sciences*, **50 (13)**, 1841–1864.

Howell, J. and J. Sun, 1999: Surface layer fluxes in stable conditions. *Boundary-Layer Meteorology*, **90**, 495–520.

Mahrt, L., 1999: Stratified atmospheric boundary layers. *Boundary Layer Meteorology*, **90**, 375–396.

Nakamura, R. and L. Mahrt, 2005: A study of intermittent turbulence with cases-99 tower measurements. *Boundary-Layer Meteorology*, **114**, 367–387.

Nieuwstadt, F., 1984: The turbulent structure of the stable, nocturnal boundary layer. *Journal of the Atmospheric Sciences*, **41 (14)**, 2202–2216.

Nieuwstadt, F., 2005: Direct numerical simulation of stable channel flow at large stability. *Boundary-Layer Meteorology*, **116**, 277–299.

ReVelle, D., 1993: Chaos and 'bursting' in the planetary boundary layer. *Journal of Applied Meteorology*, **32**, 1169–1180.

Salmond, J., 2005: Wavelet analysis of intermittent turbulence in a very stable nocturnal boundary layer: implications for the vertical mixing of ozone. *Boundary-Layer Meteorology*, **114**, 463–488.

Smedman, A.-S., 1988: Observations of a multi-level turbulence structure in a very stable atmospheric boundary layer. *Boundary-Layer Meteorology*, **44**, 231–253.

Sun, J., et al., 2004: Atmospheric disturbances that generate intermittent turbulence in nocturnal boundary layers. *Boundary-Layer Meteorology*, **110**, 255–279.

van de Wiel, B., A. Moene, W. de Ronde, and H. Jonker, 2008: Local similarity in the SBL and mixing length approaches: consistency of concepts. *Boundary Layer Meteorology*, in press.

van de Wiel, B., A. F. Moene, O. K. Hartogensis, H. A. R. D. Bruin, and A. A. M. Holtslag, 2003: Intermittent turbulence and oscillations in the stable boundary layer. part III: A classification for observations during cases99. *Journal of the Atmospheric Sciences*, **60**, 2509–2522.

van de Wiel, B., A. F. Moene, R. J. Ronda, H. A. R. D. Bruin, and A. A. M. Holtslag, 2002a: Intermittent turbulence and oscillations in the stable boundary layer. part II: A system dynamics approach. *Journal of the Atmospheric Sciences*, **59**, 2567–2581.

van de Wiel, B., R. Ronda, A. Moene, H. de Bruin, and A. Holtslag, 2002b: Intermittent turbulence and oscillations in the stable boundary layer over land, part I: A bulk model. *Journal of the Atmospheric Sciences*, **59**, 942–958.

Webb, E., 1970: Profile relationships: the log-linear range, and extension to strong stability. *Quarterly Journal of the Royal Meteorological Society*, **96**, 67–90.

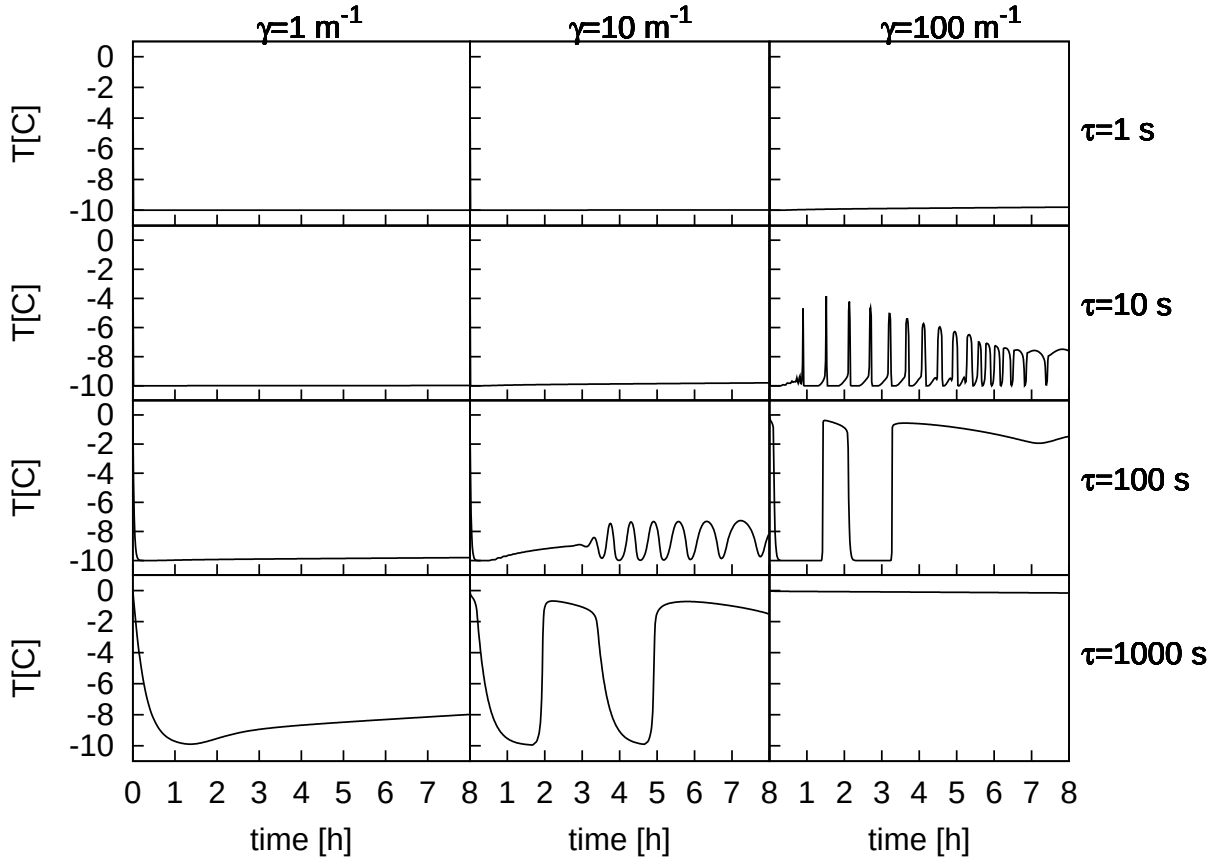

Figure 3: A logarithmic view of the influence of the parameters τ and γ for $T_g = -10C$. The transition from radiative nights to turbulent nights is seen from top left to right bottom. The unsteady intermittent behaviour is in between this transition. The intermittent behaviour is aperiodic and has a decaying trend.

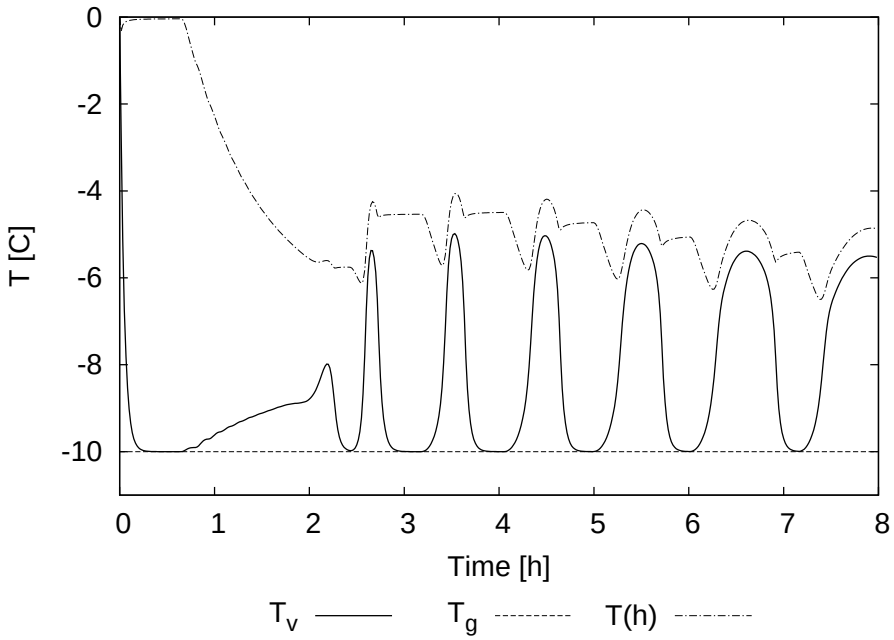

Figure 4: The figure shows the timeseries of T_{veg}, $T\left(h\right)$ and T_g for $\gamma = 10$, $\tau = 150$ and $T_g = -10$. The temperature T_{veg} and $T\left(h\right)$ have an aperiodic, oscillating behaviour. A change between fully laminar states $(T_{\mathrm{veg}} = T_g)$ is interchanged with burst of turbulent states, where the coupling between the surface and the atmosphere drives the temperature increase for T_{veg}.

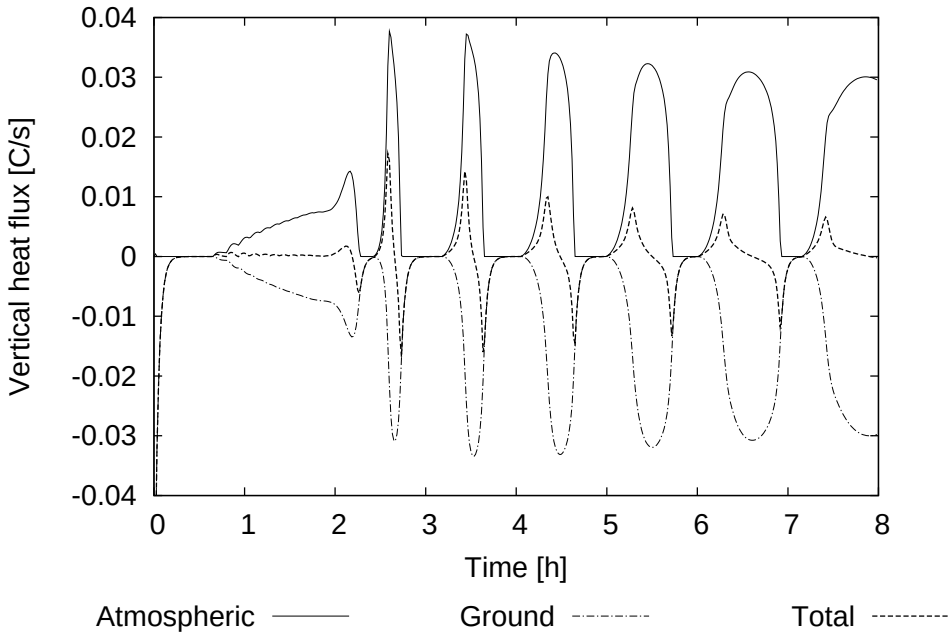

Figure 5: The time development of the ground flux $\left(-\tau^{-1}\left(T_{\mathrm{veg}} - T_g\right)\right)$, the atmospheric flux $\left(\alpha\phi\left(z_0\right)\right)$ and the sum of these two fluxes, the total flux for $\gamma = 10$, $\tau = 150$ and $T_g = -10$. The atmospheric flux is governed by the state of the atmosphere, while the ground flux is governed by the difference between T_{veg} and T_g. The lag of the response of the ground flux on changes in the atmospheric flux is governed by τ. This leads to the typical behaviour of the total flux during a burst: at the occurence a positive flux while at the decay a negative flux.

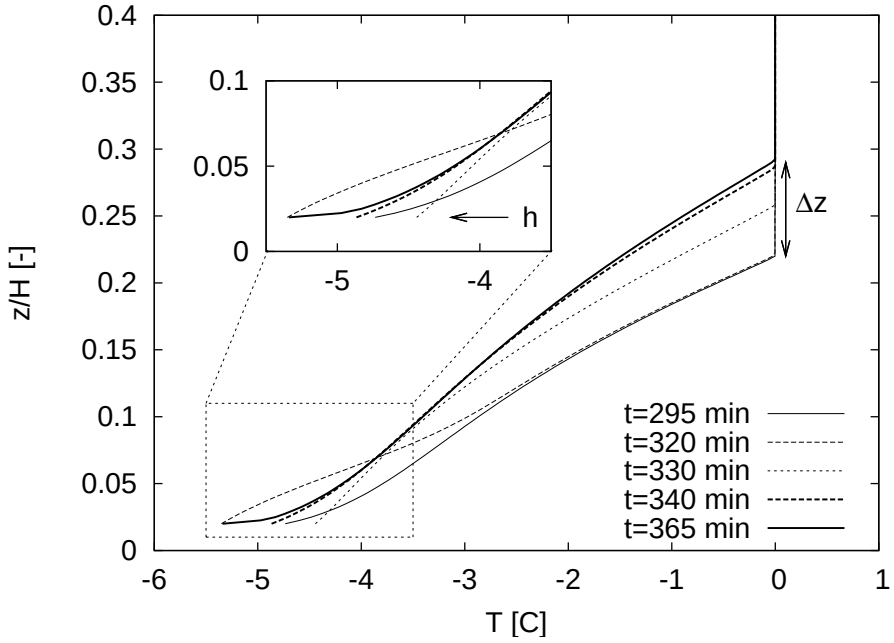

Figure 6: The time development of the temperature profiles for a single burst, burst 4 in figure 4. At $z = h$, see subfigure, we observe the characteristic behaviour of the atmospheric temperature. At first a strong decrease due to the coupling of surface and atmosphere, followed by an increase due to the entrainment of warm air. $\triangle z$ is the increase of the stable boundary layer height due to the entrainment during a single burst.

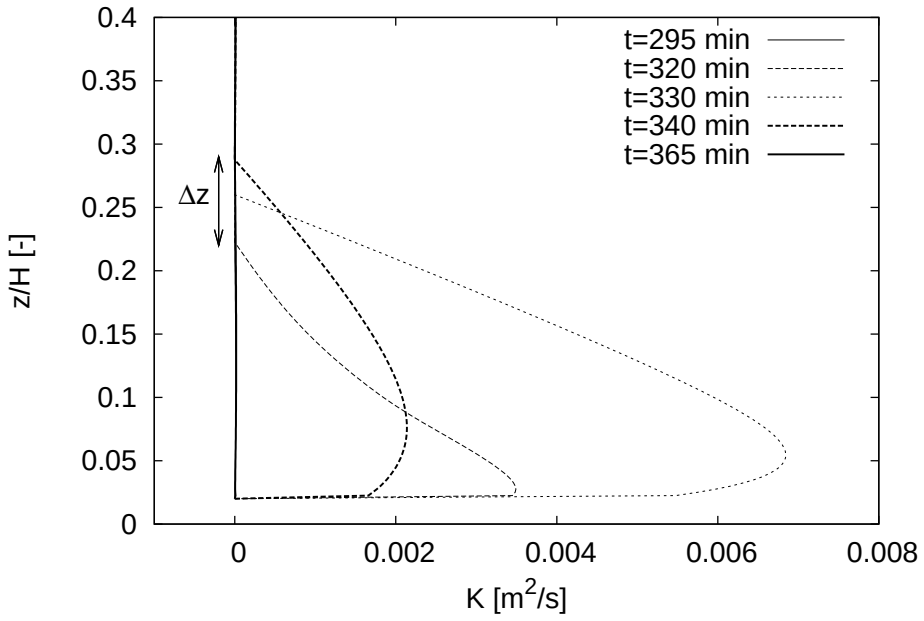

Figure 7: The time development of the K profiles for a single burst, burst 4 in figure 4. At the start of the burst the system is completely laminar ($K = 0$ for all z), due to the strong stratification ($f\,(Ri) = 0$). During the turbulence burst the stratification is overcome and turbulent viscosity arises. At the end of the turbulent burst the stable boundary layer height is increased by $\triangle z$.

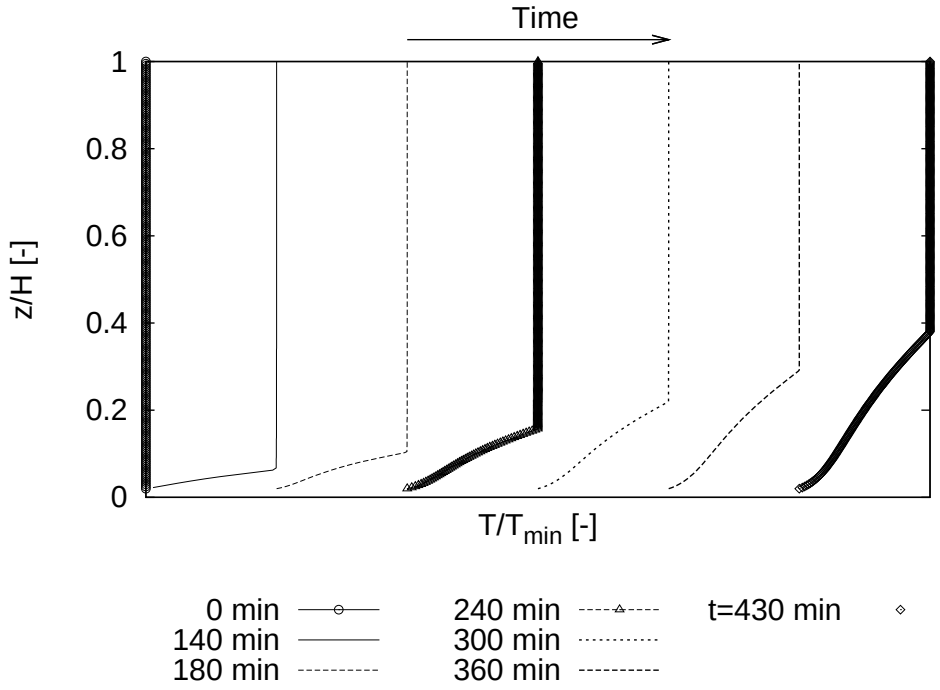

Figure 8: The time development of the temperature profiles, where each profile correspond to the midpoints between bursts in figure 4. Every profile is normalised with its own minimum ($\approx T_g$). The growth of the stable boundary layer height is observed in time due to the entrainment. We note the decrease of the stratification strength ($\partial T/\partial z$) in time. The sharp bend at the inversion height is inherent of our system, because molecular mixing is absent in our description ($\kappa = 0$).

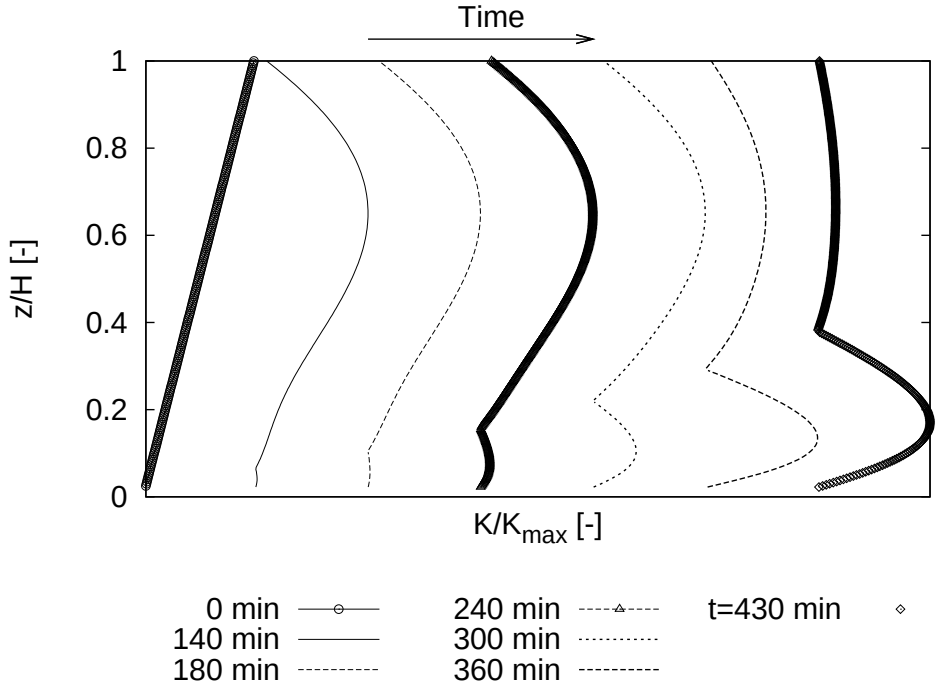

Figure 9: The time development of the turbulent diffusivity K profiles, where each profile correspond to the midpoints between bursts in figure 4. Every profile is normalised with its own maximum. Both the increase of the boundary layer height, due to entrainment, and the increase of (weak) turbulence close to the surface, due to the decrease of stratification, is shown. It is important to compare the figure with figure 7, where we observe that on an absolute scale the turbulene intensity is negligible.

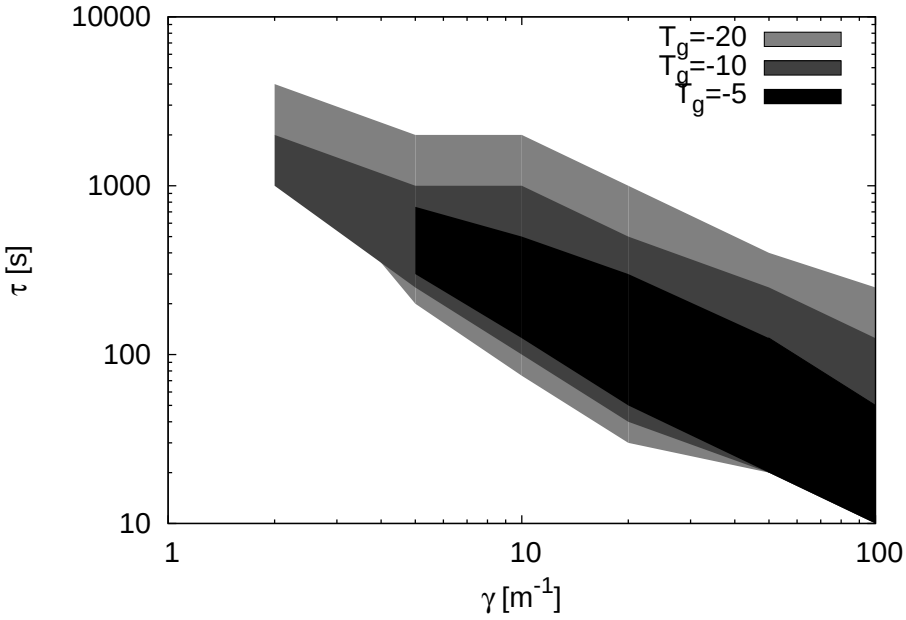

Figure 10: We show for $T_g = -5, -10$ and -20 the parameter space for γ and τ for which qualitative unsteady behaviour is observed. For $T_g = -1$ no unsteady behaviour is observed.